PREDICTING FAILURE BEHAVIOR OF POLYMERIC COMPOSITES USING A UNIFIED CONSTITUTIVE MODEL

M. J. Vallejo [*] **R. A. Tarefder** [**]

Department of Civil Engineering
University of New Mexico
Albuquerque, NM 87131, U.S.A.

ABSTRACT

This study predicts the failure behavior of an IM7/977-2 carbon epoxy composite material through a unified constitutive model. The traction-separation response and damage initiation and evolution behavior were studied by modeling a composite double cantilever beam subjected to a Mode I delamination. Damage within the composite panels was also taken into consideration through the use of the disturbed state concept (DSC). The finite element modeling software Abaqus was used to model the failure behavior of the composite using a unified constitutive modeling approach. The finite element model was validated by comparing the model results to referenced laboratory testing performed on IM7/977-2 carbon epoxy composite. The results of the finite element modeling performed in this study are in good agreement with the referenced laboratory testing. The damaged states associated with various stages of loading are presented in this study.

Keywords : Polymeric composite, Unified constitutive model, Double cantilever beam, Finite element model, Delamination.

1. INTRODUCTION

Composite materials are widely used in the space industry today. Composites have been used extensively in the construction of space equipment such as spacecraft, missiles, satellites, and launch components. In particular, polymeric composites have been extensively used due to the composite's light weight and performance under adverse environmental conditions. In order to determine the design life of the composite material used in such applications, an accurate prediction of the failure behavior of the material is required.

The macroscale failure of composite materials has been described through the traditional methods of classical damage mechanics and through a fracture mechanics approach. Classical damage models involve the plastic deformation in a damaged zone of the composite material. This damaged zone is described through a decrease in the stiffness (elastic modulus) of the material. In addition to a reduced stiffness value, the damaged zone possesses no strength. The drawback to classical damage models is that a damaged zone and an undamaged zone within the composite material must be pre-defined; there is therefore no interaction between the damaged and undamaged zones within the composite material.

Fracture mechanics assumes that the damage to the material is large enough to be described through a discrete fracture which has a macroscale geometry. The geometry of the crack affects the behavior of the material. The description of failure through fracture mechanics models involves the definition of cracks at a specific location within the composite material, or the definition of the locations of failure zones within the material. This limits the failure analysis of the composite material since the failure zones must be predefined.

The behavior of composite materials has thus far been largely described through continuum mechanics or fracture mechanics. To date, very little research has been performed which combines the failure behavior of a composite material into a single unified approach, which is done in this study.

2. OBJECTIVES AND SCOPE

The objective of this study is to use a single unified constitutive modeling approach which allows the prediction of the failure behavior of carbon-epoxy composite panels without having to define a damaged and undamaged zone; rather, any part of the composite material is allowed to fail based on the current stress state in the material. The unified model describes the failure behavior of two composite panels in a double cantilever beam configuration under an applied displacement and realistically determines the type of failure that

[*] Research fellow [**] Assistant Professor, corresponding author

DOI : 10.1017/jmech.2011.40

Copyright © 2011 The Society of Theoretical and Applied Mechanics, R.O.C.
https://doi.org/10.1017/jmech.2011.40 Published online by Cambridge University Press

the composite experiences. Specifically, the various stages of failure are described as the composite material is loaded. First, the model describes the elastic behavior of the composite panels and the cohesive zone between the panels under loading. As the load increases, the model describes the damaged material behavior in two parts; first, damage to the composite panels according to the disturbed state concept (plastic deformation, microvoid nucleation, growth and coalescence), and second, damage at the interface between the composite panels, which obeys a traction-separation law. Finally, as the load reaches a critical stage, the model describes complete separation at the interface between the composite panels and ultimate failure.

The unified model which describes all stages of composite behavior under a load are described using the principle of the disturbed state concept (DSC), which provides a unified approach for the constitutive modeling of materials deforming under a load (Sane, *et al*, [1], Desai [2]). The disturbed state concept describes the change in a material subjected to a load as it progresses to the failed state. The DSC approach accounts for the stress state within the material, the stress path that the deforming material follows, and the volume change the material may experience by microcracking and fracturing which is described through a disturbance factor. Thus, the DSC approach describes the entire failure behavior of the material as it is loaded in a unified approach. Materials behavior in DSC is described below.

3. MATERIAL DAMAGE AND FAILURE

Material failure is defined as the complete loss of load-carrying capacity that results from progressive degradation of the material stiffness (Abaqus [3]). Material failure can be described through two steps: Damage initiation, which is a criterion at which damage within the material begins, and through damage evolution, which is described through a decrease in the elastic modulus of the material. The evolution of damage within a material can then be described through the stress-strain curve of the material as shown in Fig. 1.

The undamaged response of the material is shown through line *abcd* in Fig. 1, where line *ab* represents the linear elastic behavior of the material, line *bc* represents plastic yielding with strain hardening. Line *cd*′ represents the state of the material without damage. If the material is damaged however, a different stress-strain path is created. Point *c* defines the state of the material at which damage begins. The damage then evolves along line *cd*, which is described through a damage evolution law whereby the material stiffness degrades under the applied stress. Point *d* is then the point at which the stiffness of the material has fully degraded.

The damage evolution of a material describes how the material degrades after a damage initiation criterion is met. Damage evolution can be described as the total displacement (for elastic materials) or plastic displacement (bulk elastic-plastic materials) after damage

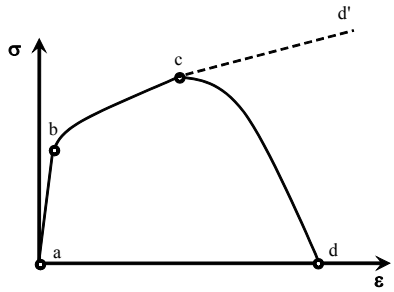


Fig. 1 Stress-Strain Curve for a Damaged Material (Abaqus [3])

initiation; this process is referred to as displacement damage evolution. Damage evolution can also be described as the amount of energy required for a material to fail (fracture energy) after damage is initiated; this is referred to as energy damage evolution. The overall damage of a material can be described through a generalized damage equation as shown in Eq. 1:

$$\sigma = (1 - D_e)\,\bar{\sigma} \tag{1}$$

where σ = stress during loading, D_e = the overall damage variable, and $\bar{\sigma}$ is the stress within the material if the material is not damaged. This damage variable approach is the cornerstone of the disturbed state concept of unified modeling and captures the overall failure behavior of the material. The material is unable to carry a load at a damage value of $D_e = 1$.

4. TRACTION-SEPARATION LAWS

The interface between lamina is of key importance to the mechanical performance of a composite such as IM7/977-2 (Hyer, [4]). The interface between lamina affects the mechanical behavior of the composite under loading. The interface may serve as an initial weak zone from which damage initiates. The behavior of the matrix material at the laminate interface can be described through continuum-based modeling, where the interface material is assumed to have a finite dimension and distinct material properties, or through traction-separation-based modeling, where the material at the interface is very thin and has a geometric thickness that may be considered as zero (Abaqus [3]). Traction-separation-based modeling is commonly used for composite materials since the size of the lamina interface is at the nanoscale.

Separation can occur at the lamina interface through loads which cause the lamina to peel apart, or loads which cause the lamina to shear apart. In the case of linear elastic traction-separation response, the composite interface material follows a linear elastic behavior when loaded until a critical load is reached. When the load is reached, damage is initiated. The nominal stress experienced by the composite at the interface is linearly related to the nominal strains at the interface. If the constitutive thickness of finite elements at the

https://doi.org/10.1017/jmech.2011.40 Published online by Cambridge University Press

interface is assumed to be equal to unity, then the nominal strain experienced by the composite is equal to the separation at the interface. The elastic response of the material can be described as shown in Eq. 2:

$$t = K\varepsilon = \begin{Bmatrix} t_1 \\ t_2 \\ t_3 \end{Bmatrix} = \begin{bmatrix} K_{11} & K_{12} & K_{13} \\ K_{21} & K_{22} & K_{23} \\ K_{31} & K_{32} & K_{33} \end{bmatrix} \begin{Bmatrix} \varepsilon_1 \\ \varepsilon_2 \\ \varepsilon_3 \end{Bmatrix} \quad (2)$$

In Eq. 2, t is the nominal traction stress vector where t_1, t_2, and t_3 = traction stress within a composite during loading in the 1, 2, and 3 principal coordinate directions (the fiber direction, perpendicular to the fiber direction (shear direction), and transverse perpendicular to the fiber direction (transverse shear direction)). The normal, shear, and transverse shear strains within the material are represented by ε_1, ε_2, and ε_3, respectively. K represents the elasticity matrix of the material and relates the traction stress vector to the strain vector. As the loading sequence continues, damage evolves at the interface, and the capacity of the interface material to sustain a load is reduced until the material has been completely damaged.

5. DAMAGE INITIATION

Damage is described through damage mechanics principles which predict damage in a material through the growth of voids and joining of voids within a material. Damage initiation can also mark the starting point of the degradation of the material at the lamina interface.

5.1 Damage Initiation for Composite Panels

The failure behavior of the composite panels examined in this study was modeled according to the disturbed state concept (DSC), which describes the change in a material subjected to a load as it progresses to the failed state. This is primarily expressed as a decrease in the modulus of the material and a corresponding decrease in the load-carrying capacity of the material, which is caused by the growth and coalescence of voids within the material. This principle is similar to the definition of ductile damage as described by Abaqus [3], where the stress within the material is decreased by a disturbance factor.

The constitutive model which describes damage initiation according to ductile fracturing and the DSC assumes that the equivalent plastic strain at the onset of damage, $\bar{\varepsilon}_D^{pl}$, is related to the stress triaxiality (the ratio of the pressure stress to the Mises equivalent stress) and the strain rate. Damage is then initiated when the ductile criterion shown in Eq. 3 is met (Abaqus [3]):

$$\omega_D = \int \frac{d\,\bar{\varepsilon}^{pl}}{\bar{\varepsilon}_D^{pl}(\eta, \bar{\varepsilon}^{pl})} = 1 \quad \text{or:}\ D_i = 1 \quad (3)$$

where ω_D = a state variable which describes plastic deformation, $\bar{\varepsilon}^{pl}$ = the plastic strain, $\bar{\varepsilon}_D^{pl}$ = the equivalent plastic strain at the onset of damage, and h = stress triaxiality = $-p/q$ = ratio of the pressure stress to the Mises equivalent stress, where $p = -1/3\sigma_{ii}$ and $q = \sqrt{\frac{3}{2} S_{ij}\, S_{ij}}$. Di is the damage initiation variable; when $Di = 1$, damage within the material is initiated.

5.2 Damage Initiation at Interfaces

When failure of a composite material is assumed to occur at the interface and a traction-separation assumption is also made, it is necessary to define the point at which damage initiates. The stress and strain required for failure at the lamina interface can be determined through the concept of traction and separation. With this concept, the geometric thickness of the interface is assumed to be zero, and the constitutive thickness of elements at the interface is assumed to be equal to one. This allows for the assumption that the strains at the interface are equal to the relative separation displacements between two lamina. This concept is described as follows (Diehl, [5]).

Nominal stress within the laminate interface is defined as the force component divided by the original finite differential area of an element of interface material. Nominal strain is the separation between lamina at the interface divided by the original constitutive thickness of the interface. In order to model the stress-strain response of the composite panels specifically at the interface, the constitutive thickness of the interface material, h_{eff}, is assumed to be equal to one. This ensures that the strain calculated at the interface is equal to the displacement on either side of the interface. The strain at the interface can then be written as shown in Eq. 4:

$$\varepsilon = \frac{\delta}{h_{eff}} \quad (4)$$

where ε = strain at the interface of the composite, δ = displacement between the laminates on either side of the interface, and h_{eff} = initial constitutive thickness of the interface material. The strain can also be expressed through the three components of composite strain: ε_1, ε_2, and ε_3 with corresponding directional displacements δ_1, δ_2, and δ_3. Using this concept, the traction-separation response can be described as shown in Fig. 2.

In Fig. 2, $t°$ represents the peak stress within the composite and the point at which damage is initiated. This peak traction stress can be specified for the local 1, 2, or 3 directions of the composite material ($t°_1$, $t°_2$, or $t°_3$). The symbol $\delta°$ represents the displacement associated with the peak traction stress. This displacement can be in the local 1, 2, or 3 directions of the composite ($\delta°_1$, $\delta°_2$, and $\delta°_3$). Because the initial constitutive thickness, h_{eff}, can be set to a value of 1, the displacements represent the strain at the interface in the respective principal material coordinate directions. As the material is loaded, there is an increase in stress and a corresponding increase in displacement between the laminates at the interface boundary until a critical value (δ^f) is reached.

https://doi.org/10.1017/jmech.2011.40 Published online by Cambridge University Press

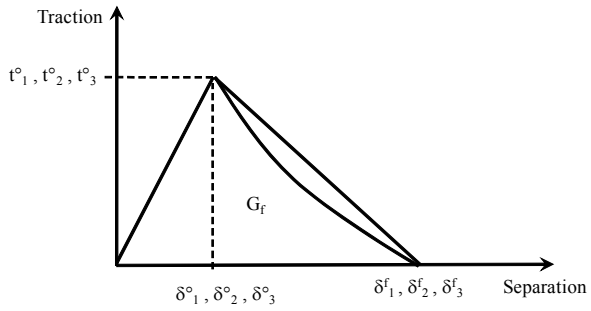


Fig. 2 Traction-Separation Response of a Composite Material

5.3 Maximum Nominal Stress Damage Initiation

In order to define the peak value at which damage begins, several maximum traction stress criterion can be established. If a maximum nominal traction stress criterion is established, damage initiates when the nominal traction stress ratio reaches a value of 1 as shown in Eq. 5 (Abaqus [3]):

$$\max\left\{\frac{<t_1>}{t_1^\circ}, \frac{t_2}{t_2^\circ}, \frac{t_3}{t_3^\circ}\right\} = 1 \quad \text{or}: \ D_i = 1 \tag{5}$$

where t_1, t_2, and t_3 = traction stress within a composite during loading in the 1, 2, and 3 principal coordinate (normal, shear, and transverse) directions; and t° = peak stress at which damage is initiated. The Macaulay brackets < > in Eq. 5 signify that a purely compressional deformation in the fiber direction of the composite will not initiate damage. D_i is the damage initiation variable; when D_i = 1, damage within the material is initiated.

The initiation of damage can also be described through a quadratic combination of the traction stresses in the principal material directions as shown in Eq. 6 (Abaqus [3]):

$$\left\{\frac{<t_1>}{t_1^\circ}\right\}^2 + \left\{\frac{t_2}{t_2^\circ}\right\}^2 + \left\{\frac{t_3}{t_3^\circ}\right\}^2 = 1 \quad \text{or}: \ D_i = 1 \tag{6}$$

5.4 Maximum Nominal Strain Damage Initiation

Damage initiation may also be modeled through a maximum nominal strain criterion by specifying a strain value at which damage is initiated. A normal, shear, or transverse shear maximum strain value can be utilized as initiation criteria, and damage is initiated when the nominal traction strain value reaches unity, as shown in Eq. 7 (Abaqus [3]):

$$\max\left\{\frac{<\varepsilon_1>}{\varepsilon_1^\circ}, \frac{\varepsilon_2}{\varepsilon_2^\circ}, \frac{\varepsilon_3}{\varepsilon_3^\circ}\right\} = 1 \quad \text{or}: \ D_i = 1 \tag{7}$$

where ε_1, ε_2, and ε_3 = strain within a composite during loading in the 1, 2, and 3 principal coordinate directions; and ε° = peak strain value at which damage is initiated.

The initiation of damage can also be described through a quadratic combination of the strains in the principal material directions as shown in Eq. 8 (Abaqus [3]):

$$\left\{\frac{<\varepsilon_1>}{\varepsilon_1^\circ}\right\}^2 + \left\{\frac{\varepsilon_2}{\varepsilon_2^\circ}\right\}^2 + \left\{\frac{\varepsilon_3}{\varepsilon_3^\circ}\right\}^2 = 1 \quad \text{or}: \ D_i = 1 \tag{8}$$

6. DAMAGE EVOLUTION

After damage in a composite material has been initiated, a damage evolution path can be specified to describe how damage proceeds and the point where ultimate failure is reached.

6.1 Damage Evolution for Composite Panels

Damage evolution according to the DSC is similar to ductile damage in that damage is described through softening of the yield stress and degradation of the elasticity of the material (Abaqus [3]). Damage evolution is described in Fig. 3.

In this figure, E = elastic modulus of the material, D_e = damage evolution variable, σ_0 = yield stress at the onset of damage, ε_0^{pl} = equivalent plastic strain at the onset of damage, and ε_f^{pl} = equivalent plastic strain at failure. In Fig. 3, the solid portion of the curve represents the damaged material stress-strain response, while the dashed line represents the undamaged material response. The damage evolution variable D_e describes the effect of the damage mechanisms acting on the material. When D_e reaches a value of 1, damage evolution is complete, and the material can no longer sustain any stress.

If a finite element approach is used to model damage evolution, the equivalent plastic strain at failure, $\bar{\varepsilon}_f^{pl}$, is a function of the finite element length and thus cannot be used as a material parameter to describe damage evolution. Damage evolution can then be described through fracture energy dissipation, G_f, which is defined as the energy required to open a unit area of crack within the composite panel (Abaqus [3]). The response of the material after damage is initiated is then described through a stress-displacement response instead of a stress-strain response as shown in Eq. 9:

$$G_f = \int_{\bar{\varepsilon}_0^{pl}}^{\bar{\varepsilon}_f^{pl}} L \times \sigma_y \times d\,\bar{\varepsilon}^{pl} = \int_0^{\bar{u}_f^{pl}} \sigma_y \times d\,\bar{u}^{pl} \tag{9}$$

where G_f = fracture energy dissipation, $\bar{\varepsilon}_0^{pl}$ = equivalent plastic strain at the onset of damage, and $\bar{\varepsilon}_f^{pl}$ = equivalent plastic strain at failure, L = characteristic length of the finite element, σ_y = yield stress, $\bar{\varepsilon}^{pl}$ = the plastic strain rate, $\bar{u}^{pl}$ = equivalent plastic displacement, and $\bar{u}_f^{pl}$ = equivalent plastic displacement at failure. The characteristic length L in Eq. 9 is based on the geometry of the finite element. For solid elements, L is the cube root of the integration point for volume; for shells and planar elements, L is the square root of the integration point area.

https://doi.org/10.1017/jmech.2011.40 Published online by Cambridge University Press

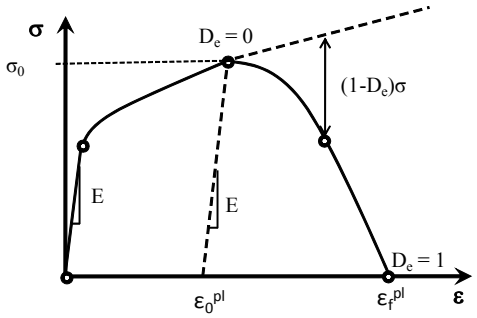


Fig. 3 Parameters for the Stress-Strain Curve of a Damaged Material

6.2 Damage Evolution at Interfaces

Damage evolution for traction-separation behavior can be more specifically described through the traction stresses at the laminate interface and the separations experienced at the laminate interface. This is shown in Fig. 2. In Fig. 2, t° represents the peak traction stress within the composite, which can be a traction stress in the local 1, 2, or 3 directions. This represents a critical value at which damage is initiated. Beyond this value, the traction stress increases while the separation (displacement) increases until a failed separation value, δ^f, is reached. This path can be described as a linear or exponential damage evolution curve. The damage evolution of the material can be described through the damage variable, which reduces the amount of traction stress that the material can bear. This is described in Eq. 10:

$$\begin{aligned} t_1 &= (1-D_e)\,\bar{t}_1 \\ t_2 &= (1-D_e)\,\bar{t}_2 \\ t_3 &= (1-D_e)\,\bar{t}_3 \end{aligned} \tag{10}$$

where t_1, t_2, and t_3 = current traction stress within a composite during loading in the 1, 2, and 3 principal coordinate (normal, shear, and transverse shear) directions, $\bar{t}_1$, $\bar{t}_2$, $\bar{t}_3$ are the traction stresses predicted by the linear elastic traction-separation behavior without damage, and D_e is the damage evolution variable.

The failed separation value, δ^f, defines the point at which damage evolution is complete and the damage evolution variable, D_e, as described by Desai [2] is equal to one. The point at which damage evolution is complete can be specified through the use of the fracture energy, G_C, required to open a unit area of crack within the interlaminar material. The fracture energy is a composite material property and is equivalent to the area under the traction separation curve shown in Fig. 2. If the area under the curve, G_C, is specified, and if the traction stress at damage initiation is known, then the point at which damage evolution is complete ($D_e = 1$) is specified.

7. METHODOLOGY

Traction-separation response and damage initiation and evolution were studied in a composite material composed of IM7 carbon graphite fibers in a 977-2 epoxy matrix. The IM7/977-2 composite was modeled in Abaqus finite element software using two laminate panels subjected to double cantilever beam loading. Finite element input parameters were based on an interlaminar toughness study of IM7/977-2 composite beam by Johnson *et al*. [6]. In this study, the Mode I interlaminar fracture toughness ("peeling" toughness) of an 8-ply, $[0_3/\pm3/0_3]$ layup composite panel and 16-ply, $[0_7/\pm3/0_7]$ composite panel subjected to double cantilever beam loading were determined through laboratory testing at various temperatures (Johnson *et al*. [6]). The experimental temperatures ranged from −196°C (−320°F) to 160°C (−20°F). The laboratory tests performed by Johnson *et al*. [6] were conducted according to ASTM D 5528-01, "Standard Test Method for Mode I Interlaminar Fracture Toughness of Unidirectional Fiber-Reinforced Polymer Matrix Composites"[7]. The finite element modeling input parameters used in this study are based on the laboratory test results of the 8-ply panel at room temperature from the Johnson *et al*. [6] study.

As specified in the Johnson study, each panel is 150mm long, 26mm wide and is 4 plys thick. Each ply is 0.150mm thick for a total panel thickness of 0.6mm. The composite geometry is shown in Fig. 4.

In the delamination laboratory experiment, a Teflon strip was inserted between the ±3 layers when the composite panels were manufactured. The Teflon strip provided an initial delamination within the composite where equipment was used to peel the panels apart. This delamination was reproduced in the present finite element study in order to directly compare the laboratory test results with finite element analysis results. A 38mm wide delamination was used in the composite model within Abaqus as shown in Fig. 5. A total displacement of 110mm was applied in the 3-principal direction of the composite layup. In order to simulate a double cantilever beam, the left edge of the composite was constrained from translation in the 1, 2, and 3 principal directions. The delamination and boundary conditions of the composite beam are shown in Fig. 5.

8. MATERIAL PROPERTIES

Two sets of material properties were used in the finite element analysis performed in this study. The first set consists of the composite panel material properties; the second set consists of the interface material properties. These properties are described in detail in the following sections.

8.1 Material Properties: Composite Panels

8.1.1 Elastic Behavior

The properties of the IM7 carbon fibers and the 977- 2 epoxy matrix used in the finite element analysis were obtained from the Hexcel® IM7 data sheet [8] and the Cycom® 977-2 data sheet [9], respectively. The properties

https://doi.org/10.1017/jmech.2011.40 Published online by Cambridge University Press

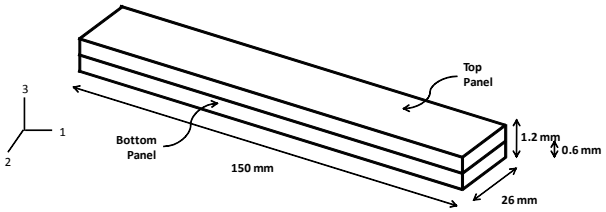


Fig. 4 Geometry of Composite for Finite Element Analysis

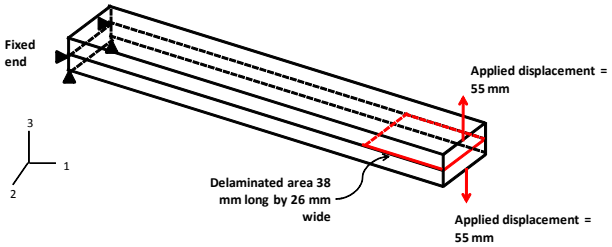


Fig. 5 Boundary and Loading Conditions for Finite Element Analysis

of the composite panels as a whole were determined using micromechanics principles with an assumed fiber-volume fraction of 60%. The elastic properties of the IM7/977-2 composite panels are summarized in Table 1.

8.1.2 Plastic Behavior

The plastic behavior of the composite panels was based on a study by Parry and Al-Hazmi [7]. In this study, cylinders of composite material composed of IM7 carbon fibers and 977-2 epoxy matrix were loaded dynamically in compression at a high strain rate of $850s^{-1}$. A stress-strain curve for the material was then developed with the test data. According to this curve, the elastic and plastic behavior of the composite material is as shown in Table 2.

8.1.3 Damage Initiation and Evolution

The initiation and evolution of damage in the composite panels was modeled using the DSC/ductile criterion shown in Eq. 3. The DSC/ductile damage was described through a decrease in stress triaxiality and fracture strain. The strain at which fracture was initiated was determined from the study by Parry and Al-Hazmi [10]. The strain rate of $850s^{-1}$ obtained from the same study was used in the ductile damage initiation parameters. The damage initiation parameters for the composite panels are summarized in Table 3.

Once damage within the composite panels was initiated, the damage evolution was described through the fracture energy required to open a unit area of crack within a composite panel, G_f. The damage evolution portion of the composite panels' stress-strain curve was assumed to be linear. A critical fracture energy of 0.478 mJ/mm^2 was used in the analysis based on the fracture energy provided in the Cycom® 977-2 Toughened Epoxy Resin data sheet [9].

Table 1 Material Properties of IM7/977-2 Composite Beam

Fiber Volume Fraction	60%
Tensile Modulus, E_1	167GPa
Transverse Modulus, E_2	7.39GPa
Transverse Modulus, E_3	7.39GPa
Poisson's Ratio, ν_{12}	0.34
Poisson's Ratio, ν_{13}	0.34
Shear Modulus, G_{12}	2.96GPa
Shear Modulus, G_{13}	2.96GPa

Table 2 Compressive Stress-Strain Properties of IM7/977-2 Composite Beam

Stress, MPa	Total Strain, %	Elastic Strain, %	Plastic Strain, %
0	0	0	0
857	1.01	1.01	0
904	1.135	1.006	0.129
943	1.265	1.059	0.206
991	1.419	1.032	0.387

Table 3 Damage Initiation Parameters for Composite Panels

Stress Triaxiality, η	Damage Initiation Strain	Strain Rate, s^{-1}
0	0.01451	850
0.1	0.008	850
0.2	0.004	850
0.3	0.002	850
0.4	0.001	850
0.5	0.0008	850

8.2 Material Properties: Interlaminar Material

The undamaged interlaminar material properties were based on the critical fracture energy of the composite material as described by Diehl [5]. A Mode I "peeling" critical fracture energy of 0.2973 mJ/mm^2 was used based on the findings by Johnson *et al.* [6] for an 8-ply double cantilever beam tested at room temperature. The interface strength of the composite was then determined using the critical fracture energy as shown in Eq. 11:

$$t^{\circ} = \frac{2G_C}{\delta^f} \tag{11}$$

where t° = interface strength of the composite material in a given principal direction, G_c = interlaminar critical fracture energy, and δ^f = cohesive ductility value as described by Diehl [5]. According to Diehl, the cohe-

https://doi.org/10.1017/jmech.2011.40 Published online by Cambridge University Press

sive ductility value, δ^f, is a function of the cohesive finite element length, L_c, and a fraction, f, of the cohesive element size. A cohesive element length of 0.2mm and a fraction of the cohesive element size of 0.5 was used in this analysis. The cohesive ductility value, δ_f, was then calculated using Eq. 12:

$$\delta^f = f\ L_C \tag{12}$$

where δ^f = cohesive ductility value, L_c = cohesive element size, and f = fraction of the cohesive element size.

The initial elastic behavior of the interface was expressed as an initial material stiffness per unit area as described by Diehl [5]. This elastic behavior is applicable to a material which obeys a traction-separation constitutive model. The initial elastic behavior was calculated as shown in Eq. 13:

$$K_{eff} = \frac{2G_C}{\delta_{ratio}(d^f)^2} \tag{13}$$

where K_{eff} = initial material stiffness per unit area, G_c = interlaminar critical fracture energy, δ^f = cohesive ductility value, and δ_{ratio} = damage initiation ratio = $\delta°/\delta^f$. The value $\delta°$ is the separation distance at which damage is initiated. Diehl [5] recommends a damage initiation ratio of 0.5 for finite element analysis. The effective elastic modulus of the interlaminar, cohesive material was then calculated using Eq. 14:

$$E_{eff} = K_{eff}\ h_{eff} \tag{14}$$

where E_{ff} is the effective elastic modulus of the cohesive interlaminar material, K_{eff} is the initial material stiffness per unit area, and h_{eff} is the initial constitutive thickness of the cohesive element as described by Diehl [5]. An initial effective thickness value, h_{eff}, of one was specified in the Abaqus finite element model used in this study. The full interlaminar properties used in this analysis are summarized in Table 4.

Table 4 Inter-laminar Material Properties of Composite

Interlaminar critical fracture energy, G_c	0.2973mJ/mm^2
Cohesive element size, L_c	0.2mm
Fraction of the cohesive element size, f	0.5
Cohesive ductility value, δ^f	0.1
Damage initiation ratio, δ_{ratio}	0.5
Interface strength,	5.95MPa
Interface stiffness, K_{eff}	118.9MPa
Effective elastic modulus, E_{eff}	118.9MPa

Table 5 Time Step Increments Used in Abaqus Finite Element Model

Maximum Number of Increments	2500
Initial Increment Size	1×10^{-4}
Minimum Increment Size	1×10^{-15}
Maximum Increment Size	0.1

9. ELEMENT TYPE AND TIME STEP

Quadrilateral continuum shell elements were used to model the IM7/977-2 composite panels. The interface of the composite was modeled using eight-noded, three dimensional cohesive elements. The time step increments used in the loading sequence in the Abaqus finite element modeling were reduced in order to account for non-linear effects. The time step increments utilized in the analysis are summarized in Table 5. Several Abaqus settings were utilized in order to control non-linear effects caused by large displacements, discontinuous finite element analysis.

10. RESULTS AND DISCUSSIONS

Several results were obtained from the finite element analysis performed on a double cantilever IM7/977-2 beam using the Abaqus software. A contour plot of the displacement in the 3-principal direction during delamination is shown in Fig. 6. A contour plot of the stress (σ_{33}) within the composite is shown in Fig. 7. The contours in the following figures have been exaggerated for ease of visibility.

In order to compare the results from this study to the laboratory experiments performed by Johnson *et al.* [6], a force versus displacement curve at a specific reference point was also generated for the composite assembly as shown in Fig. 9. The results shown in the curve represent the normal force and associated displacement at the same location where results were measured in the Johnson study; specifically, the point is located where the 55mm displacement was applied to the top composite panel. The reference point is shown in Fig. 8.

The normal force increased linearly with increasing displacement until a maximum force of 35.5N was reached at the reference point and the quadratic combination of traction stresses within the interface material reached a value of one as described in Eq. 6. Damage was initiated in the interface material after the maximum force was achieved, which also marked the starting point at which damage evolution began, and the force decreased as displacement increased.

A contour of the damage initiation criteria as described in Eq. 6 is shown in Fig. 10. The red contours indicate that the quadratic combination as described in Eq. 6 reached a value of unity, which indicates that the element reached the maximum traction stress value.

In order to determine the maximum force that could be applied to the end of the double cantilever beam before damage initiation, a plot of the damage initiation variable D_i versus force applied to the end of the beam was created as shown in Fig. 12. The force shown on the x-axis of this plot represents the force applied at the reference point located at the end of the beam as shown in Fig. 8. The damage initiation variable D_i shown on the y-axis of the plot is from an inter-laminar cohesive element at the reference location presented in Fig. 11. As shown in Fig. 12, damage is initiated in interfacial elements when the applied force at the reference element reaches a value of 17.2N; this caused the

https://doi.org/10.1017/jmech.2011.40 Published online by Cambridge University Press

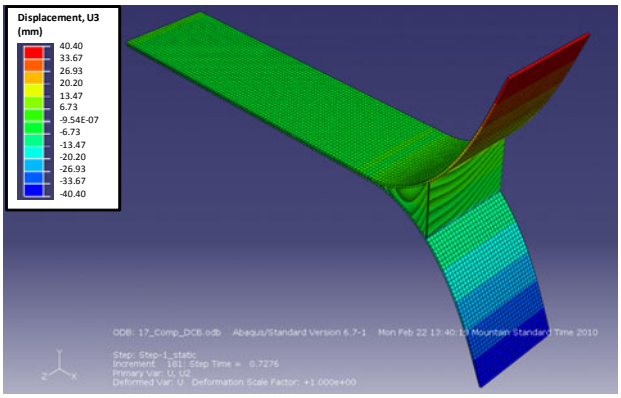


Fig. 6 Contour Plot of Displacement of the Composite Double Cantilever Beam

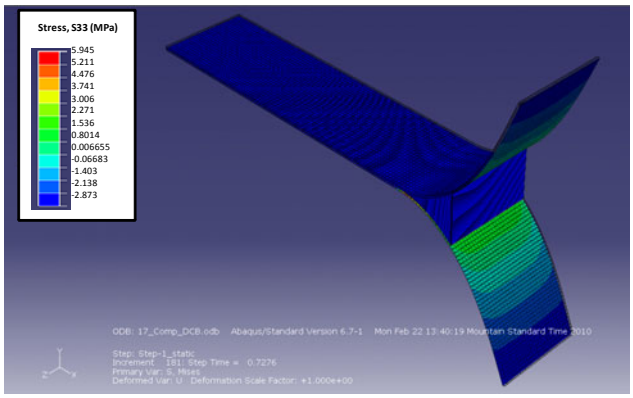


Fig. 7 Contour Plot of Stress (σ_{33}) in the Composite Double Cantilever Beam

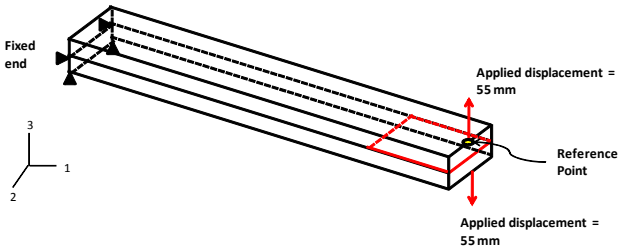


Fig. 8 Reference Point for Force and Displacement Shown in Fig. 9

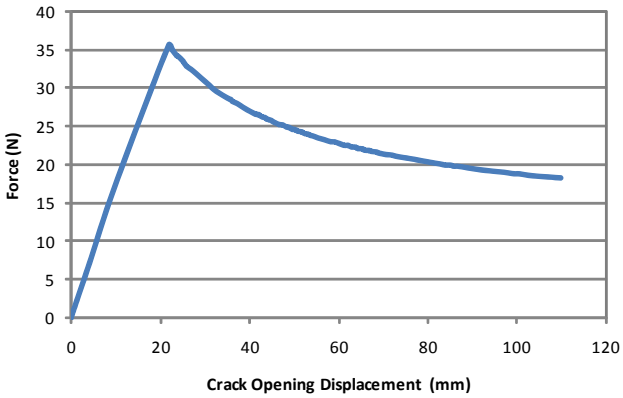


Fig. 9 Force vs. Displacement Curve for Reference Point on IM7/977-2 Beam

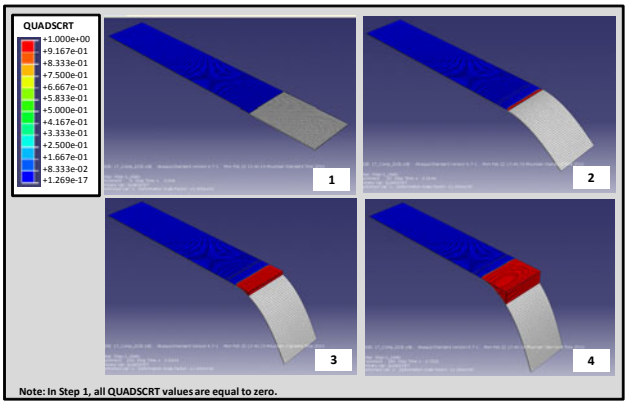


Fig. 10 Damage Initiation Variable Contour Plots for Various Time-Steps in the Loading Sequence of the Double Cantilever Beam

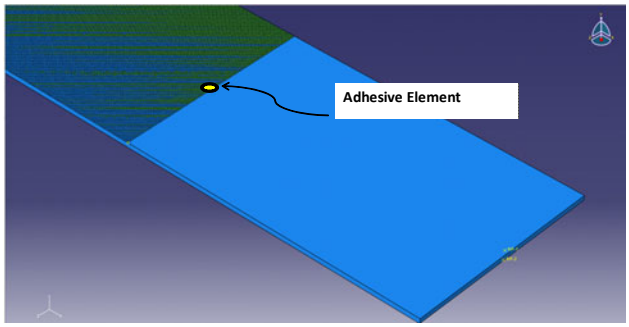


Fig. 11 Reference Element for Results Shown in Fig. 12 through Fig. 14

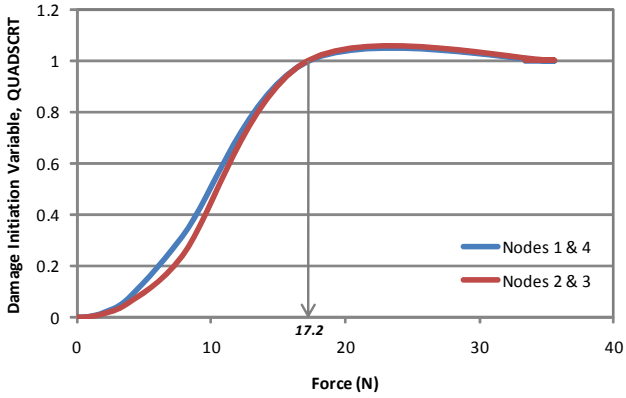


Fig. 12 Damage Initiation Variable versus Applied Force for the Nodes of an Interface Element

quadratic combination of traction stresses as described in Eq. 6 to reach a value of one ($D_i = 1$). The damage evolution variable D_e versus the force applied to the end of the beam is shown in Fig. 13.

After damage was initiated when the applied force reached 17.2N, the traction stress that the interlaminar elements were able to sustain was reduced according to the damage evolution law described in Eq. 10. The disturbed state damage variable D_e was reduced linearly by equating the area under the traction-separation curve to the fracture energy required to open a unit area of interlaminar crack, G_C as shown in Table 4. The damage variable was increased until it reached a value equal to one; beyond that point, the interlaminar

https://doi.org/10.1017/jmech.2011.40 Published online by Cambridge University Press

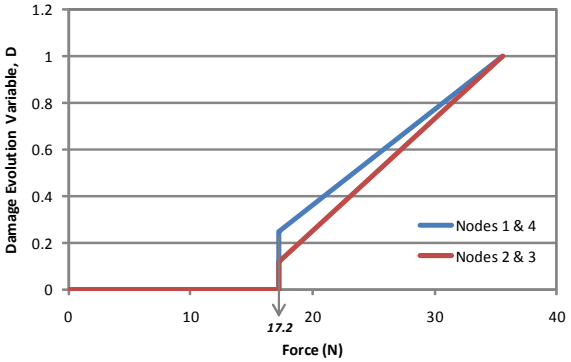


Fig. 13 Damage Evolution Variable versus Applied Force for the Nodes of an Interface Element

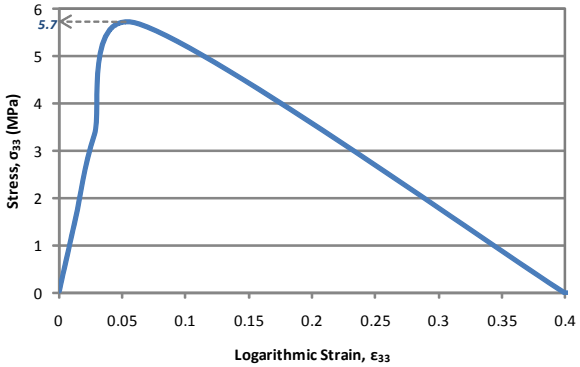


Fig. 14 Stress σ_{33} versus Strain ε_{33} in Interface Material

elements could no longer sustain a traction force, and the elements completely failed. This process continued until the entire composite beam experienced delamination. The evolution of damage in an element of the interface material in terms of stress and logarithmic strain is shown in Fig. 14. The location of the interface element is shown in Fig. 11. As can be seen from this curve, the damage evolution portion is linear. As shown in Fig. 14, a maximum quadratic stress value of 5.7MPa was reached within the interface material. The stresses that the interlaminar elements were able to maintain were then systematically reduced until the elements could no longer sustain stress.

The results obtained in the finite element modeling performed in the present research were compared to the laboratory test results of the interlaminar toughness study of an IM7/977-2 composite beam (Johnson *et al.* [6]). The force versus displacement curve obtained during laboratory testing for an 8-ply, $[0_3/\pm3/0_3]$ layup composite panel at room temperature are shown in Fig. 15.

In the current study, a maximum force of 35.5N with an associated displacement of 21.9mm was obtained from the Abaqus finite element model. This result is in agreement with the maximum force of 32.3N obtained from the laboratory testing of an 8-ply, $[0_3/\pm3/0_3]$ layup IM7/977-2 composite panel performed by Johnson *et al*. [6]. The associated displacement obtained in the Johnson *et al*. [6] laboratory testing was 10.5mm. However, the authors believe that the displacement specified in the Johnson laboratory testing represents the displacement of only one composite panel (half of the total displacement). The total associated displacement obtained in the Johnson *et al*. [6] laboratory testing is therefore 21mm, which is in agreement with the results obtained in the present study. Thus, the finite element model developed in this study correlates well with the laboratory test results obtained during the Johnson experiment.

The damage initiation versus force curve shown in Fig. 12 may be used to predict the force at which damage will occur in the interface of an IM7/977-2 composite panel subjected to peeling (Mode I loading). The damage evolution variable, D_e, versus force data shown in Fig. 13 may be used to predict the force at which damage has completely evolved and the interface of the composite material can no longer sustain a force.

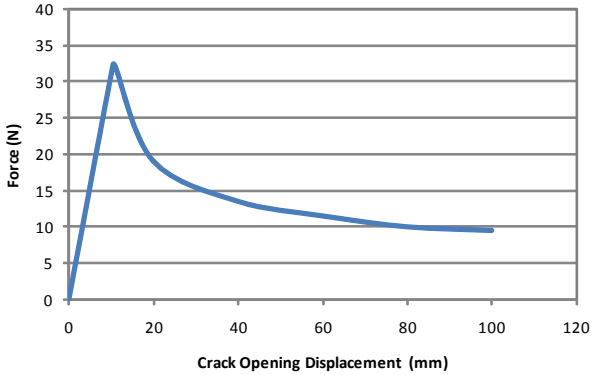


Fig. 15 Force vs. Displacement Curve for IM7/977-2 Double Cantilever Beam according to Johnson *et al.* [6]

10.1 Damage to Composite Beams

A contour plot of the DSC/ductile damage initiation variable is shown in Fig. 16. As shown in this figure, damage was not initiated in the top or bottom composite panels under the applied displacement. This result was expected, as the strength of the composite panels was much larger than that of the interface material. The stress-strain curve for a reference element on the composite panel is shown in Fig. 17. This reference element is located on the top composite panel just above the interface material reference element shown in Fig. 11.

As shown in Fig. 17, the stress state of the bottom side of the top composite panel reached a maximum tensile stress of 833MPa with an associated strain of 4.95×10^{-3}. The top side of the top panel reached a compressive stress of negative 833MPa. This stress state indicates that the composite panels did not reach the failure stress specified in Table 3; thus, damage was not initiated in the composite panels.

11. CONCLUSIONS

This study focuses on a double cantilever beam composed of IM7/977-2 composite material subjected to Mode I loading. The developed finite element model predicts the interlaminar strength of the

https://doi.org/10.1017/jmech.2011.40 Published online by Cambridge University Press

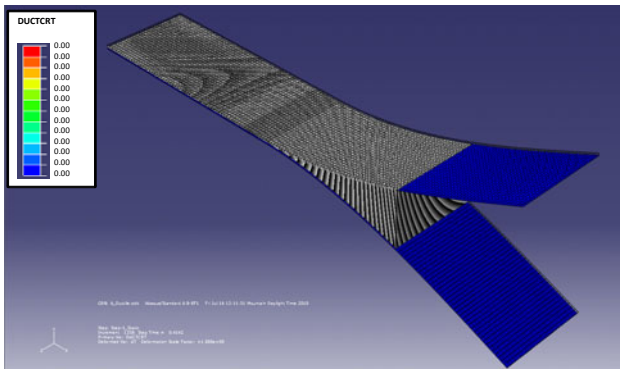


Fig. 16 Ductile Damage Initiation Variable Contour Plot for Double Cantilever Beam

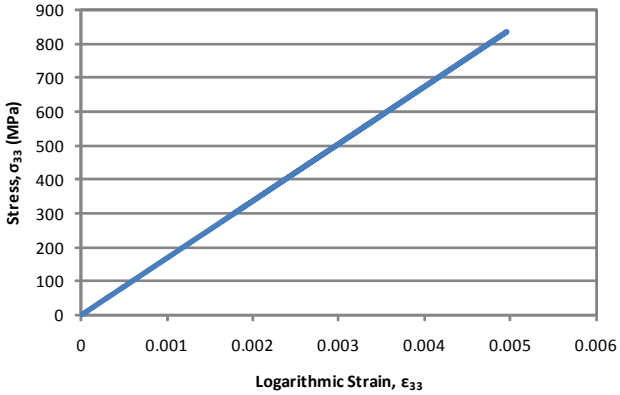


Fig. 17 Stress σ_{33} versus Strain ε_{33} in Top Composite Panel Element

IM7/977-2 composite with reasonable accuracy as compared to laboratory data obtained from Johnson *et al.* [6]. According to the results of the finite element model, damage within the interlaminar material of an 8-ply, IM7/977-2 composite panel at room temperature will occur at an applied Mode I "peeling" force of 35.5N with an associated displacement of 21.9mm. Damage evolution can then be described according to a traction-separation law as shown in Fig. 14.

Damage within the composite material was described in a unified manner without pre-defining a cracked zone in this study. Damage was described according to a damage variable, *D* according to the disturbed state concept. The stiffness and load-carrying capability of the interface material was systematically reduced according to a traction separation law until the interface material could not sustain a load and completely failed.

ACKNOWLEDGEMENTS

This project is funded by the New Mexico Space Grant Consortium and NASA-EPSCoR, grant number: 456-254. The authors would like to express sincere gratitude towards Ms. Judy McShannon, and Dr. Pat Hynes, Director of New Mexico Space Grant Consortium and NASA EPSCoR. Thanks to Professor C.S. Desai of University of Arizona for their assistance in DSC and unified constitutive modeling.

REFERENCES

1. Sane, S. M, Desai, C. S., and Jenson, J. W., *et al.,* "Disturbed State Constitutive Modeling of Two Pleistocene Tills," *Quaternary Science Reviews*, **27**, pp. 267–283 (2008).
2. Desai, C. S., "Mechanics of Materials and Interfaces: The Disturbed State Concept," CRC Press LLC (2001).
3. Abaqus Analysis Users Manual, v. 6.7, Dassault Systemes (2007).
4. Hyer, M. W., "Stress Analysis of Fiber-Reinforced Composite Materials," *Second Edition*, DEStech Publishers Inc., Lancaster, PA (2008).
5. Diehl, T., "On Using a Penalty-Based Cohesive-Zone Finite Element Approach, Part I: Elastic Solution Benchmarks," *International Journal of Adhesion and Adhesives*, **28**, pp. 237–255 (2008).
6. Johnson, W. S., Pavlick, M. M. and Oliver, M. S., "Determination of Interlaminar Toughness of IM7/977-2 Composites at Temperature Extremes and Different Thicknesses," *Final Report*, NASA Grant Number NAG-1-02003 (2005).
7. "Standard Test Method for Mode I Interlaminar Fracture Toughness of Unidirectional Fiber-Reinforced Polymer Matrix Composites," American Society for Testing and Materials (ASTM) (2007).
8. Hexcel® HexTow® IM7 Carbon Fiber Product Data Sheet, accessed on 2/11/2010. http://www.hexcel.com/NR/rdonlyres/BD219725-D46D-4884-A3B3-AFC86020EFDA/0/HexTow_IM7_5000.pdf.
9. Cycom® 977-2 Toughened Epoxy Resin Data Sheet, http://www.cytec.com/engineered-materials/products/Cycom977-2.htm (February 11, 2010).
10. Parry, D. J. and Al-Hazmi, F. S., "Stress-Strain Behavior of IM7/977-2 and IM7/APC2 Carbon Fibre Composites at Low and High Strain Rates," *Journal de Physique*, **110**, pp. 57–62 (2003).

(Manuscript received March 3, 2010,
accepted for publication September 23, 2010.)

https://doi.org/10.1017/jmech.2011.40 Published online by Cambridge University Press